Chemical Engineering Journal 406 (2021) 126796

Contents lists available at ScienceDirect

Chemical Engineering Journal

journal homepage: www.elsevier.com/locate/cej

Erythritol-based polyester loose nanofiltration membrane with fast water transport for efficient dye/salt separation

Pengrui Jin[a], Junyong Zhu[b,*], Shushan Yuan[a], Gang Zhang[c], Alexander Volodine[d], Miaomiao Tian[a], Jianxiu Wang[a], Patricia Luis[e], Bart Van der Bruggen[a,f,*]

[a] Department of Chemical Engineering, KU Leuven, Celestijnenlaan 200F, B-3001 Heverlee, Belgium
[b] School of Chemical Engineering and Energy, Zhengzhou University, Zhengzhou 450001, PR China
[c] Institute of Materials Science and Technology, Sichuan University, Chengdu 610064, PR China
[d] Laboratory of Solid-State Physics and Magnetism, Department of Physics and Astronomy, KU Leuven, Celestijnenlaan 200D, B-3001 Leuven, Belgium
[e] Materials & Process Engineering (iMMC-IMAP), UC-Louvain, Place Sainte Barbe 2, 1348 Louvain-la-Neuve, Belgium
[f] Faculty of Engineering and the Built Environment, Tshwane University of Technology, Private Bag X680, Pretoria 0001, South Africa

HIGHLIGHTS

- The novel polyester loose nanofiltration membranes were fabricated by interfacial polymerization method.
- The optimized polyester membrane exhibited excellent water permeability.
- This polyester membrane exhibited both a high rejection of dyes and a high transmission of salts.
- This polyester membrane showed a superior antifouling performance and long-term stability.

ARTICLE INFO

Keywords:
Loose nanofiltration
Meso-Erythritol
Polyester
Interfacial polymerization
Dye/salt separation

ABSTRACT

Loose nanofiltration membranes with a remarkable water permeability are highly promising for the fractionation of dyes and salts in the treatment of textile wastewater. In this study, a novel polyester membrane with unprecedented water permeability was developed via interfacial polymerization (IP), in which meso-erythritol (ME) was utilized as an aqueous monomer. Instead of using toxic catalysts, sodium hydroxide was incorporated to the aqueous solution to catalyze the ester reaction between hydroxyl and acyl chloride. A series of characterizations demonstrated that the formed polyester film is hydrophilic and negatively charged, with microsphere structures on the surface. Due to the low-active hydroxyl groups of the aqueous monomers, the participation of ME could yield a coherent polyester film with slightly loose structure atop the polyethersulfone (PES) membrane. The resultant membrane with high water permeability exhibited both a high rejection of dyes and a high transmission of salts. The rejection of the LNFM-2 membrane with an excellent water permeability of 53.23 LMH bar^{-1} for Congo red (CR), direct red 23 (DR23), reactive blue 2 (RB2), Na_2SO_4, NaCl was 99.6%, 95.2%, 99.6%, 11.0%, and 5.6% respectively. Furthermore, LNFM-1 has a water permeability of up to 87.13 LMH bar^{-1} while maintaining a competitive dye/salt separation performance. In addition, this type of polyester membrane has a superior antifouling performance and long-term stability during the filtration of dye/salt mixtures.

The newly developed polyester LNF membranes have great application potential in the treatment of textile wastewater. This study paves the way for applying hydroxyl monomers like polyols for constructing TFC membranes for diverse separations.

1. Introduction

Dyes have been widely used in the textile, plastics, paper and other industries for decades [1]. However, a large amount of colored wastewater is produced during the dyeing process, which not only pollutes the environment but also threatens human health [2]. Generally, a large amount of inorganic salts, mainly sodium chloride, is used during the dye synthesis process [3]. In order to boost the uptake of dyes by the fibers, some inorganic salts such as sodium chloride (~6.0 wt%) and sodium sulfate (~5.6 wt%) are introduced within the dyeing process [4-

* Corresponding authors at: Department of Chemical Engineering, KU Leuven, Celestijnenlaan 200F, B-3001 Heverlee, Belgium (B. Van der Bruggen).
E-mail addresses: zhujunyong@zzu.edu.cn (J. Zhu), bart.vanderbruggen@kuleuven.be (B. Van der Bruggen).

https://doi.org/10.1016/j.cej.2020.126796
Received 1 April 2020; Received in revised form 20 August 2020; Accepted 22 August 2020
Available online 27 August 2020

6]. Thus, either the formation of salt by-products in the dye synthesis or artificial addition of salts in the dyeing procedure will inevitably lead to the coexistence of dyes and salts in textile wastewater. Nonetheless, the excessively high salt concentration in dye wastewater complicates conventional treatment processes, such as adsorption [7], photocatalytic treatment [8] and chemical oxidation [9], making the dye/salt mixtures complicated to be separated and recovered. From the concept of sustainable development, textile wastewater treatment requires a mode upgrade, not only for traditional filtration (such as reverse osmosis, dye exclusion or pure water production), but also for the recovery of resources (including salts and dyes) from textile water. Overall, the fractionation of dye/salt mixtures is of pivotal importance for desalination of dye solutions and for dye reuse and purification.

Nanofiltration (NF) membranes with a molecular weight cutoff range of 200–1000 Da and pore size about 0.5–2.0 nm are ideal candidates for the treatment of wastewater [6,10-14]. Conventional NF membranes are able to reject dyes and salts simultaneously by size sieving [15] and electrostatic repulsion (the Donnan effect) [16], rather than fractionating the dye/salt mixtures. In order to achieve the separation of dye/salt mixtures based on NF, a new concept of loose nanofiltration (LNF) was proposed to achieve the removal of organics with low molecular weight, while allowing a high permeation of inorganic salts (especially divalent salts) in 2004 [17]. Since then, substantial attempts have been made to develop loose nanofiltration for the fractionation of dye/salt mixtures [6,12,18-20].

Three main approaches have been utilized to fabricate LNF membranes: co-deposition of polyphenol-inspired monomers (such as catechol, tannic acid and dopamine) with polyethylenimine (PEI) [19,21-23], blending of functional fillers within PES matrices via phase inversion [6,12,24], in situ self-assembly to prepare hydrolyzed polyacrylonitrile (HPAN) membranes [25-27]. However, the intricate synthesis procedures and expensive raw materials largely restrict the large-scale implementation of the above-mentioned methods. Furthermore, the current strategies of improving water flux are generally at the cost of solute rejection, impeding potential applications in rapid and efficient separation of dye/salt mixtures. Therefore, it is of crucial significance to seek for cost-effective methods for developing highly selective and highly permeable LNF membranes. Interfacial polymerization (IP) is an established technique to prepare thin film composite (TFC) NF membranes with cross-linked structure [28]. In the IP process, the generation of an active thin film layer on the substrate membrane is the key to determine the performance of TFC NF membrane. The physicochemical properties of monomers play a crucial role in the pore diameter, thickness, electrical properties and hydrophilicity of the thin film layer. Therefore, TFC membranes can be designed with desired properties by the manipulation of diverse monomers. Compared to commonly used polyamide NF membranes prepared by polyamines [29-32], only few studies have been carried out to prepare the less used polyester NF membranes formed by polyols or polyphenols [33-39]. This can be caused by the lower salt rejection of the polyester NF membranes compared to polyamide NF membranes due to their loose structure formed by the hydroxyl groups in the monomers, which have a low activity [34,36,40]. For instance, Cheng et al. [34] selected pentaerythritol as aqueous monomer to construct novel polyester TFC membranes for desalination. The optimized polyester TFC membrane exhibited good rejection of Na_2SO_4 (98.1%), but only a $MgSO_4$ rejection of 67.9% and an extremely low water permeability (1.2 LMH bar^{-1}, at 25 °C). This also means that the salt rejection of a polyester TFC membrane can be greatly reduced, while the permeability is enhanced to the level of commercial polyamide TFC membrane (around 10 LMH bar^{-1}) [41]. Furthermore, polyester TFC membranes constructed via IP reaction between trimesoyl chloride (TMC) and tannic acid on a PES substrate [38] showed 56% higher water permeability (23.4 LMH bar^{-1}) than a polyamide TFC membrane constructed by piperazine and TMC via IP on a PES ultrafiltration support [42]. However, the salt rejection of polyamide TFC membrane (97.4%) was higher than that of polyester TFC membrane (50.2%). Inspired by the above results, we hypothesized that the loose structure formed by the hydroxyl groups in the polyols/polyphenols would be suitable for fractionating dye/salt mixtures. However, reported studies only focused on the excellent antifouling [33,38,39] and chlorine-resistant [34,43] properties of the polyester TFC membranes but did not notice that the loose structure of polyester TFC membranes may be suitable for the fractionation of dye/salt mixtures. To enhance the application potential of polyester TFC membranes and develop more efficient textile wastewater treatment membranes, it is important to study the filtration of dye/salt mixtures with polyester TFC membranes.

Meso-Erythritol (ME) is a compound with four hydroxyl groups, which has been broadly applied in confectionery, food products and pharmaceuticals [44,45]. Considering that its hydroxyl groups can react with acyl chloride of TMC under certain conditions, a polyester TFC NF membrane can be synthesized via an IP reaction. However, most of the hydroxyl monomers used to prepare polyester composite membranes are not active; the IP reaction requires additional catalysts or a longer reaction time to ensure a defect-free polyester film [42,43,46]. Previous studies demonstrated that the use of sodium hydroxide (NaOH) can transform polyols and polyphenols to salts, thus increasing the activity of monomers and contributing to a thin film within a shorter IP time [47,48]. Therefore, NaOH is expected to be a promising catalyst to facilitate the esterification between ME and TMC.

In this study, a novel high-flux polyester TFC LNF membrane, with intended high rejection of dyes and fast permeation of salts (even divalent salts), was prepared by the IP between ME and TMC catalyzed by NaOH on the PES substrate membrane, as shown in Fig. 1. In addition, the prepared polyester membrane with ME monomers is thought to endow the TFC LNF membrane with superior anti-fouling performance. The aim of this research is not only to report a novel synthetic approach to prepare high-flux LNF membrane, but also to emphasize that the hydroxyl-containing monomers (e.g., polyols, polyphenols) have great application potential in the field of LNF.

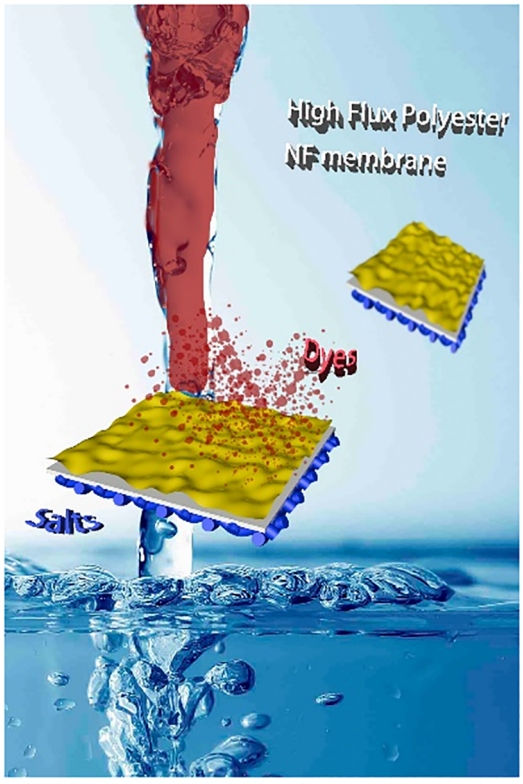

Fig. 1. Schematic diagram of polyester membrane for dye/salt filtration.

Table 1
Properties of dyes used in this study.

Dye	MW[a] (g mol^{-1})	λ[b] (nm)	Chemical structure
Congo red (CR)	696.6	498	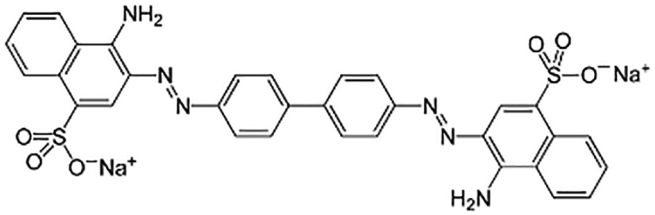
Reactive blue 2 (RB 2)	774.2	628	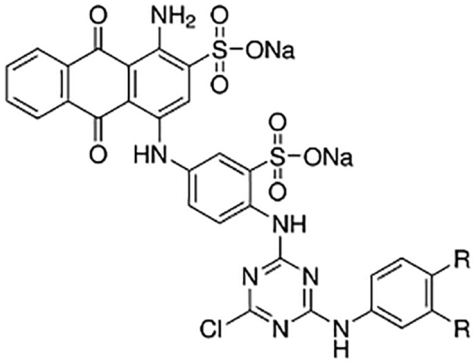 R = H or SO_3Na (one of each)
Direct red 23 (DR 23)	813.7	507	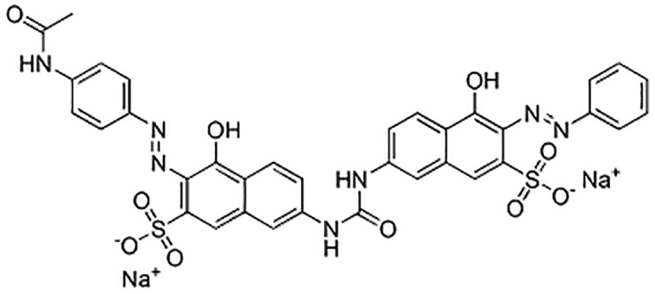

[a] Molecular weight.
[b] Maximum adsorption wavelength.

2. Experiments

2.1. Chemicals and materials

Polyethersulfone (PES) (Ultrason E3000P) was supplied by BASF Co., Ltd. Dimethyl sulfoxide (DMSO, 99.5%), Meso-Erythritol (ME, ≥99%), trimesoyl chloride (TMC, 98%), n-hexane (95%) and sodium hydroxide (NaOH, 90%) in the form of powder were purchased from Sigma-Aldrich (Belgium) to prepare polyester TFC membranes. Congo red (CR, dye content: 40%), direct red 23 (DR23, dye content: > 30%), reactive blue 2 (RB2, pure) from Sigma-Aldrich were selected to assess the rejection ability of polyester membranes at a concentration of 200 ppm; the chemical structure of these dyes is shown in Table 1. Sodium chloride (NaCl, 99%), sodium sulfate (Na_2SO_4, 99%) were supplied by Sigma-Aldrich and used for salt rejections at a concentration of 1000 ppm. All the aqueous solutions were prepared by deionized (DI) water.

2.2. Membrane preparation

2.2.1. Preparation of PES UF membranes

The PES casting solution with polymer concentration of 15.0 wt% was obtained via dissolving PES powders in DMSO via vigorous stirring at a constant room temperature of 25 °C ± 3 °C for over 10 h. The resultant casting solution was degassed in a centrifuge for 10 min at 4000 rmp, followed by using a casting knife with a thickness of 250 μm to cast it onto the surface of non-woven fabric. Subsequently, the initial membrane was placed into a water bath for solvent/nonsolvent exchange. Finally, the resultant PES membranes were stored in deionized water at 4 °C prior to use.

2.2.2. Polyester TFC NF membranes preparation procedure

IP reaction was carried out in a clean and ventilated fume hood at a constant room temperature of 25 °C ± 3 °C and a relative humidity of 33% ± 3%. As shown in Fig. 2, polyester TFC membranes were fabricated via IP between ME and TMC catalyzed by NaOH on PES substrate surfaces. Firstly, the residual water on the PES membrane surface was removed gently by an air knife; then, the PES membrane was clamped in a glass holder module and surface coated with aqueous ME/NaOH solution (20 mL) for 6 min. Afterwards, the aqueous solution was poured from the glass holder, and the redundant liquid on the membrane surface was eliminated as soon as possible. Secondly, the organic TMC/n-hexane solution (8 mL, 1 mg mL^{-1}) was poured into the membrane module to achieve the IP for different durations at a constant room temperature of 25 °C ± 3 °C. After the removal of the residual TMC solution, the membranes were washed thoroughly with DI water and then stored in DI water (4 °C) before use. Within contrast with previous studies, heat treatment after IP was not used in this work,

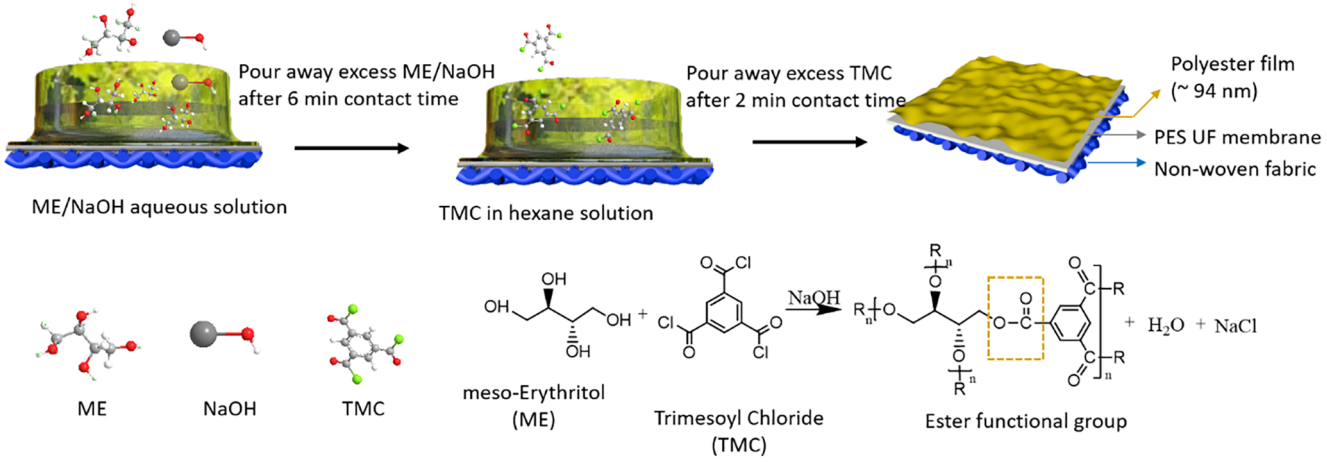

Fig. 2. Scheme of the fabrication process and IP reaction mechanism for the ME polyester membrane. R is possibly H and dicarbonyl substitution.

Table 2
The ME polyester TFC NF membranes were fabricated at various reaction time, monomer and NaOH concentrations.

Membrane	ME in aqueous phase (wt%)	NaOH in aqueous phase (wt%)	TMC in organic phase (wt%)	IP reaction time (min)
LNFM-1	**0.6**	0.5	0.1	2
LNFM-2	**0.8**	**0.5**	0.1	**2**
LNFM-3	**1.0**	0.5	0.1	2
LNFM-4	**1.2**	0.5	0.1	2
LNFM-5	**1.4**	0.5	0.1	2
LNFM-6	0.8	**0.35**	0.1	2
LNFM-7	0.8	**0.4**	0.1	2
LNFM-8	0.8	**0.45**	0.1	2
LNFM-9	0.8	**0.55**	0.1	2
LNFM-10	0.8	0.5	0.1	**1**
LNFM-11	0.8	0.5	0.1	**3**
LNFM-12	0.8	0.5	0.1	**4**

which inevitably increases the cross-link degree and thereby decreases the permeability of the polyester LNF membranes. The IP parameters, including ME concentration, the additive dosage of NaOH, and the time of IP reaction are listed in Table 2.

2.2.3. Membrane characterization

Each sample was dried in a fume hood at room temperature for over 48 h. The chemical constitution of polyester films was characterized by a NEXUS670 Fourier transform infrared (FTIR) spectrometer and Krais ULFRA x-ray photoelectron spectroscope (XPS). Surface and cross-section morphologies of polyester TFC LNF membranes were evaluated by FESEM (Philips XL30 FEG, Netherlands). Each sample was sputtered with gold (Au) before SEM observation. A dimension 3100 AFM device (Bruker USA) was utilized to determine the polyester membranes surface roughness under ambient conditions with a 10 × 10 μm^2 scanning area. The hydrophilicity of polyester membranes was evaluated by a contact angle goniometer (OCA20, Dataphysics Instruments, Germany) with 2 μL water droplets at 5 random locations. The charge properties of membrane surface were investigated using an Electrokinetic Analyzer (SurPASS 3, Anton Paar, Austria).

2.3. Filtration performance measurement

The nanofiltration performance (e.g., water permeance, dye rejection, and salt rejection) was investigated in a dead-end cell (HP4750 stirred cell, Sterlitech Crop., Kent, WA, USA) with an effective membrane area of 14.6 cm^2. Prior to filtration, all membranes were pre-pressurized at 8 bar for at least 1 h using pure water until a stable water flux was attained. In this work, the initial water permeability of LNFM-1 can reach about 280 L $m^{-2}h^{-1}$ bar^{-1}, and the permeability of after compaction is stable within 100 L $m^{-2}h^{-1}$ bar^{-1}, which may be caused by the compaction of the loose structure of a polyester film [49,50]. After compaction, the trans-membrane pressure was adjusted to 4 bar with different feeds at room temperature. The water permeability (WP, L $m^{-2}h^{-1}$ bar^{-1}) was calculated by the following equation: $WP = V/(A\hat{A}\cdot\Delta t\hat{A}\cdot\Delta p)$, where V represents the permeated solution volume (L) collected over the filtration time Δt (h), and A is the effective membrane area (m^2), Δp is the applied pressure. The retention of salts (NaCl, Na_2SO_4, 1 g L^{-1}) and dyes (CR, DR23, and RB2, 200 ppm) was calculated as $R = (1 - C_p/C_f) \times 100\%$, where C_p and C_f (g L^{-1}) are the dye/salt concentrations in the feed and permeate solution, respectively. All the dye concentrations were measured with a UV–Vis spectrometer (Shimadzu, Japan). The single salt concentrations were measured by an Electrical Conductivity equipment (Thermo Scientific Orion Star A212). In case of dye/salt mixture, before measuring the salt concentrations in the permeate, the activated carbon was employed to completely adsorb residual dyes in the permeate.

2.4. Antifouling properties test

The above performance results show that high-flux polyester membranes have potential for low-pressure operation, which can solve the problem of energy consumption due to a relative high operation pressure. Therefore, the antifouling performance of polyester TFC LNF membranes was investigated with a DR23 solution (200 ppm) at room temperature and 1 bar with the dead-end cell described above. Before recording data, the membrane was compacted with pure water to stabilize the system. The membrane was compacted with DI water to stabilize the system, then the membrane was used to filter the DI water and the data was recorded every 10 min for 1 h. The average water flux was recorded as $J_{w,1}$. Then, the feed solution was replaced by the DR23 solution for another 1 h and the average permeate solution flux was recorded as J_p. The membrane was then washed with pure water for 30 min, which was not counted in the filtration cycle. Subsequently, the pure water flux of cleaned membrane $J_{w,2}$ was measured again at the same condition. The above assessment of antifouling properties for polyester TFC LNF membranes was repeated twice. The higher flux recovery ratio (FRR) and the lower total fouling ratio (R_t) indicating the better antifouling ability of membrane can be calculated by $FRR = (J_{w,2}/J_{w,1}) \times 100\%$; $R_t = (1 - J_p/J_{w,1}) \times 100\%$. Irreversible fouling ($R_{ir}$), which can be expressed by $R_{ir} = R_t - R_r$, refers to the adsorption or deposition of molecules. Reversible fouling (Rr), which can be calculated by $R_r = (J_{w,2} - J_p)/J_1 \times 100\%$, is closely related to the fouling caused by concentration polarization.

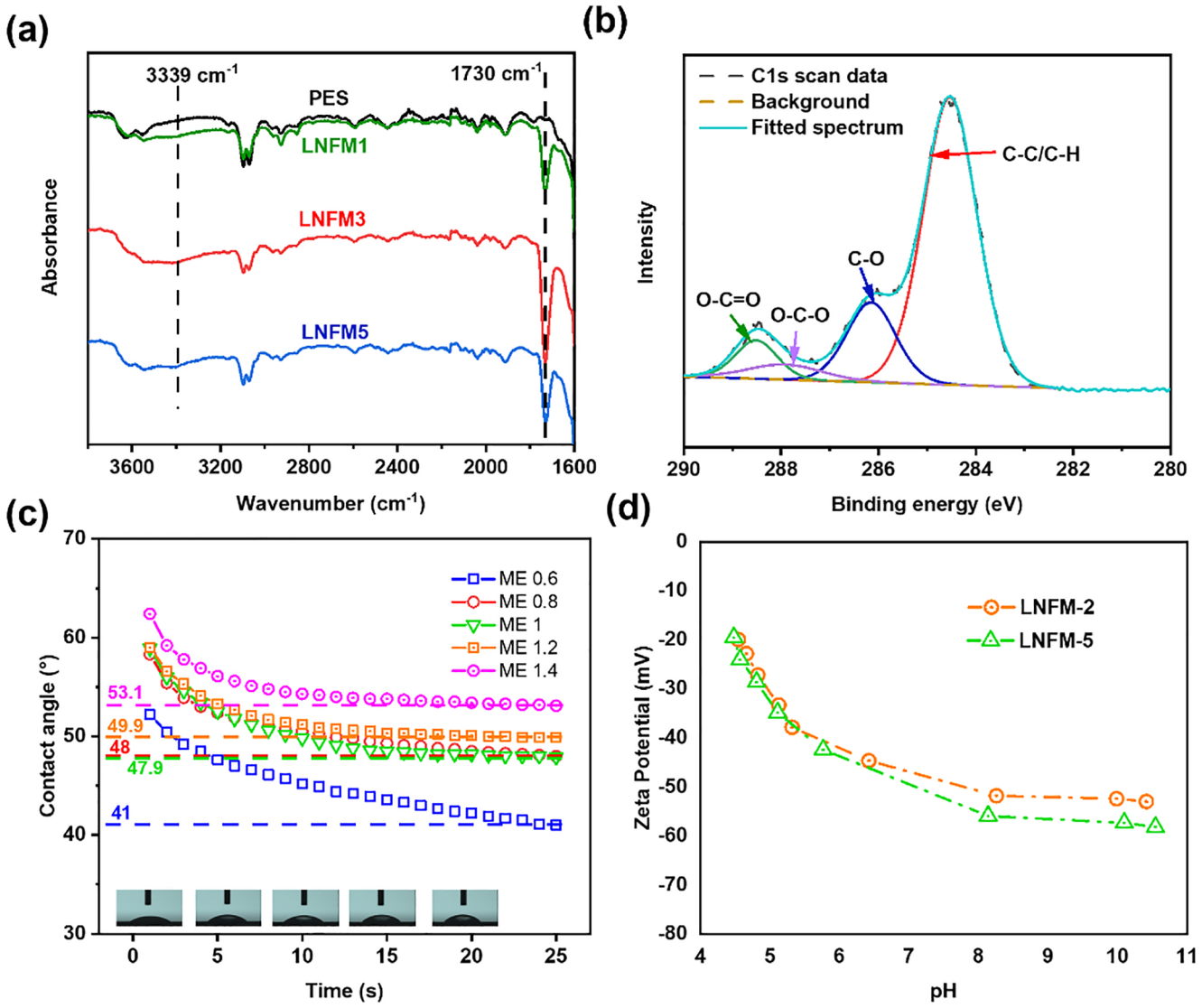

Fig. 3. (a) FTIR spectra of PES, LNFM-1, LNFM-3, and LNFM-5 membranes; (b) XPS spectra of C 1 s for the LNFM-1 membrane; (c) dynamic water contact angles of LNFM-1, LNFM-2, LNFM-3, LNFM-4 and LNFM-5 membranes; (d) zeta potentials of LNFM-2 and LNFM-5.

2.5. Dye/salt separation and stability performance evaluation

Dye/salt separation using LNFM-2 membranes were carried out in the same dead-end apparatus at 2 bar. The influence of salt concentration was observed by varying the Na_2SO_4 concentration (1, 5, 10, 20, 30 and 40 g/L) with the 200 ppm DR 23 aqueous solution. The stability of the performance of the LNFM-2 membranes was studied through a filtration test. A mixed solution containing 200 ppm DR 23 and 1 g/L Na_2SO_4 was filtered for 5 h by the dead-end system at 2 bar. Then, permeability and solution rejection were measured as mentioned before.

3. Results and discussion

3.1. Chemical structure of polyester film surface

FT-IR spectra of PES and diverse polyester TFC membranes, which were employed to analyze their surface chemical structure, are displayed in Fig. 3**a**. Different from PES substrate, the synthesized polyester film showed obvious absorption signals at 1730 cm^{-1} (C═O) and 3339 cm^{-1} (–OH). The presence of C═O groups indicates that the polyester films were successfully synthesized via the polymerization between the hydroxyl of ME and the acid chloride of TMC [43]. The broad peaks corresponding to the stretching vibration of the –OH groups are in the range of 3200–3500 cm^{-1}; hence, the new peaks were attributed to the unreacted –OH groups of ME monomers in the polyester films and carboxyl groups formed by hydrolysis of acyl chloride groups on TMC [42,47,51,52]. These unreacted hydroxyl groups and carboxyl groups are likely to advance the hydrophilicity and antifouling ability of the polyester TFC membranes, which will be discussed in **3.3** and **3.5.3**, respectively. Similar conclusions have been reported in the literature [42,43,53]. As shown in the deconvoluted C 1 s spectra of polyester TFC membranes (Fig. 3**b**), the LNFM-1 membrane displayed O-C═O, C-O, and C═O groups, which is in good agreement with the FT-IR characterization, and confirms the formation of polyester films.

3.2. Surface morphologies of composite membranes

Surface and cross-section SEM images of the polyester TFC LNF membranes are presented in Fig. 4. As can be seen from Fig. 4a-d and Fig. S1a, microsphere structures appear on the surface of the ME-LNF membrane. Moreover, it was found that the number of microspheres on the surface of ME-LNF membrane increases with the ME concentration

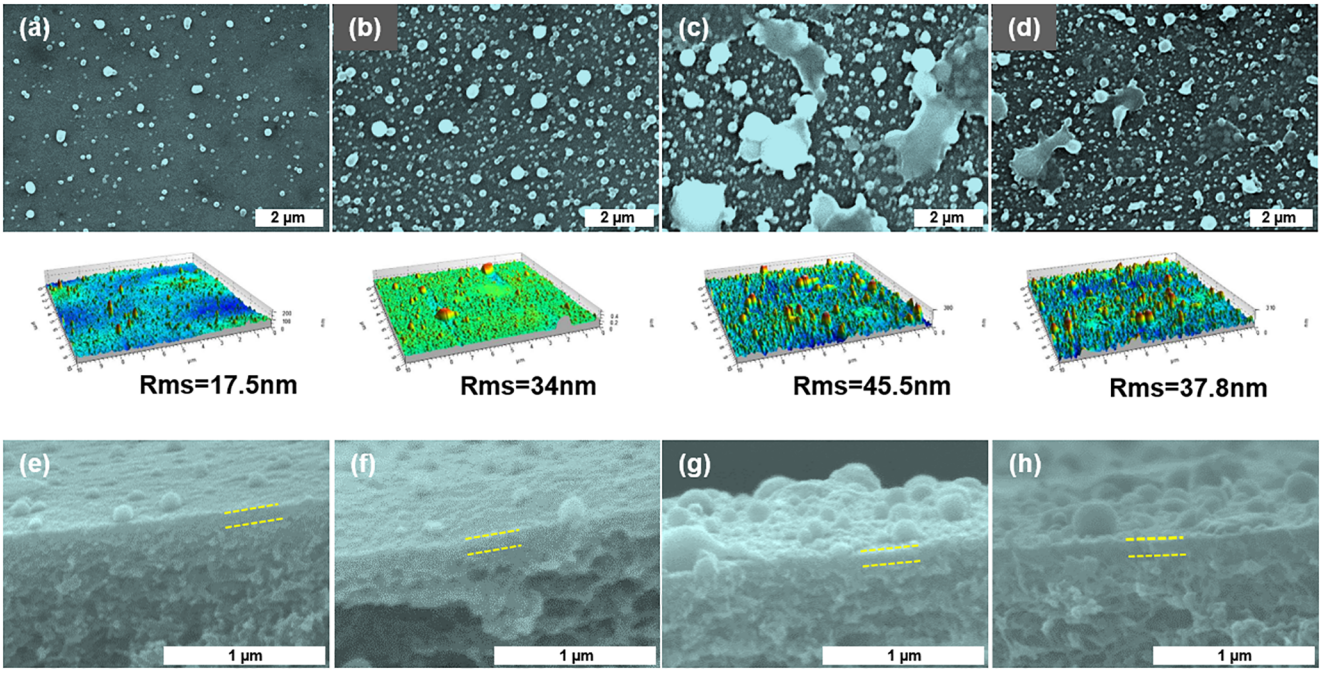

Fig. 4. The surface morphology and the root-mean-square roughness (Rms) of (a) LNFM-1, (b) LNFM-2, (c) LNFM-3, (d) LNFM-4 membranes; cross-sectional morphology of (e) LNFM-1, (f) LNFM-2, (g) LNFM-3, (h) LNFM-4 membranes.

in the aqueous phase. It cannot be ignored that the morphology of LNFM-3 is abnormal, and there is no suitable theory to explain this phenomenon at present. This may be due to the self-limiting tendency of IP [54].When the initial concentration of aqueous monomer is too high, the initial reaction rate increases, and a thin film can be formed in a shorter time, thereby limiting the diffusion of the aqueous monomer through the thin film and continuing the reaction to form a larger microsphere structure. According to the cross-sectional morphology of the polyester TFC membranes (Fig. 4 e-h and Fig. S1b), it can be observed less clearly that the thickness of the selective layer increases as the concentration of ME aqueous monomers increases. It is worth noting that many reports have confirmed that the thickness of thin film formed by IP increases with the increase of aqueous monomer concentration [55-57].

The morphology of thin films prepared via IP is influenced by the kinetic parameters, such as chemical reaction rate and diffusion rate [58]. Fig. 2 shows the mechanism of esterification crosslinking between ME and TMC catalyzed by NaOH. The monomer concentration is positively correlated with the monomer diffusion rate [59]. Thus, the high ME concentration will speed up the migration rate of ME from aqueous phase to organic phase. As a result, the reaction between TMC and ME is accelerated, which led to a high cross-linking degree [60,61]. Furthermore, the polyester film formed from the same IP reaction time showed an increase of selective layer thickness via increasing the ME concentration. In addition, the images of AFM further confirm that a low concentration of aqueous monomers leads to a relatively smooth surface with less microspheres, while the number of microsphere structures elevates with increasing concentration of aqueous monomers. This suggests that IP is a self-limiting process [47]. At the initial stage, the diffusion of ME monomers to the interface of the organic phase leads to the formation of the new polyester film. After the formation of a polyester network with a certain thickness, the diffusion channels for ME monomers are more limited. However, ME monomers with small molecules easily diffuse through the gaps and pores within the initially formed smooth selective film to form a microsphere structure on the surface at a higher monomer concentration. Thus, a rough surface with microsphere structure is formed.

3.3. Surface properties of composite membranes

A high hydrophilicity is beneficial to the improvement of permeability and anti-fouling ability of NF membranes, on which a thin layer of water is formed via hydrogen bonding between hydrophilic groups and water molecules [12]. Dynamic water contact angles (WCAs) of the polyester TFC membranes are shown in Fig. 3**c**. It was found that the initial contact angle of LNFM-1 membrane was 52.2° and declined to 41.0° after 25 s. In addition, it could be observed that the contact angle of the membranes increased considerably with increasing monomer concentration. For instance, the equilibrium value of the LNFM-5 membrane reached 53.1° when the ME concentration increased from 0.06 wt% (LNFM-1) to 0.14 wt% (LNFM-5). A lower contact angle corresponds to a higher hydrophilicity of the membranes [42]. Therefore, as the concentration of aqueous monomer increases, the hydrophilicity of the membranes decreases, but all the polyester TFC membranes have a good hydrophilicity. As described in the above FTIR results (**see 3.1**), there are carboxyl groups formed by hydrolysis of acyl chloride groups on TMC. The residual carboxylic acid groups were decreased when increasing the ME concentration for an IP reaction. Membrane surface with less polar groups or charged groups shows a weaker hydrophilicity. Thus, the hydrophilicity gradually decreased when increasing ME dosage. In addition, the accumulation of non-polar groups deriving from the ME monomers is thought to have an effect on the reduced hydrophilicity.

As displayed in the SEM images, the surface of the polyester film formed with a high ME concentration has a large number of microspheres. Since only a small amount of ME monomer can pass through the film formed in the early stage to react with a large number of TMC to form microsphere structures, the number of residual –OH groups on the ME monomers is reduced, and the hydrophilicity of the resulting polyester film is reduced.

As shown in Fig. 3**d**, zeta potential measurements were performed to better understand the surface charges that influence the membrane rejection characteristics. The polyester TFC LNF membranes exhibit a large, negative zeta potential over a wide pH range (4.5–10.5), which is primarily caused by the carboxyl groups generated from the partially cross-linked TMC monomers [42]. The residual acryl groups from

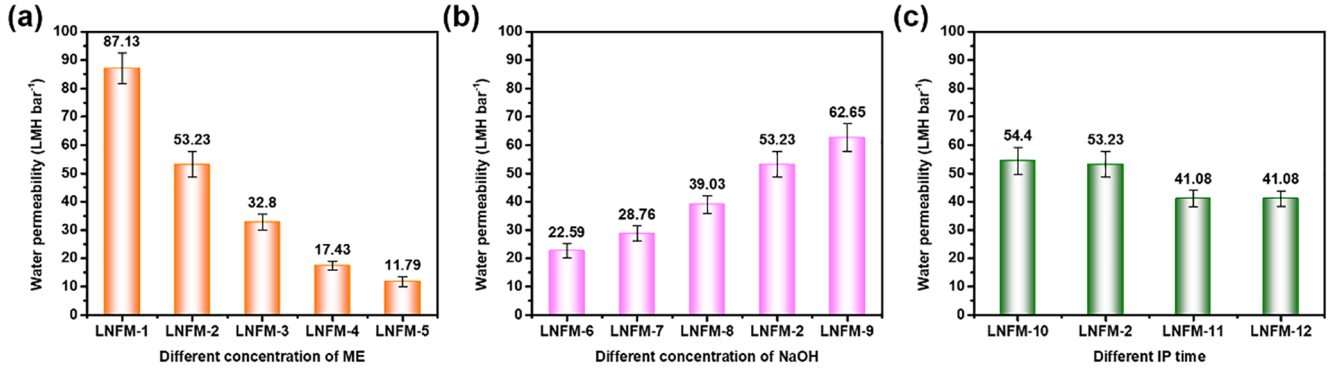

Fig. 5. DI water permeability of membranes with (a) different concentrations of ME monomer, (b) different concentrations of NaOH, (c) IP time (4 bar, 25 ± 3 °C).

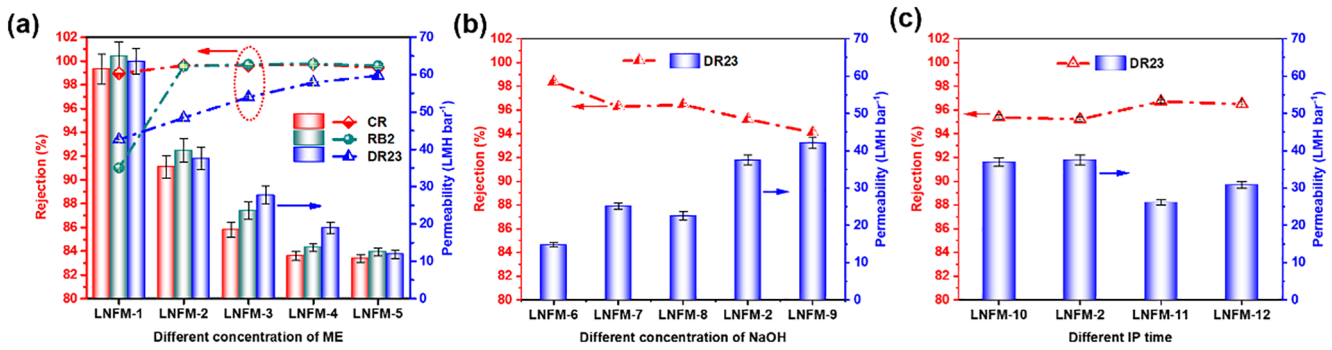

Fig. 6. Dye solution permeability and rejection of membranes with (a) different concentrations of ME monomer, (b) different concentrations of NaOH, (c) IP time (4 bar, 25 ± 3 °C).

partially cross-linked TMC were hydrolyzed into carboxylic groups after contact with water, and thus the electronegativity of the polyester TFC LNF membranes was enhanced [52,62,63]. In addition, the comparison of LNFM-2 and LNFM-5 showed that the monomer concentration in the aqueous phase has little influence on the electrical charge of the polyester TFC LNF membranes. The zeta potential results showed that the prepared polyester membranes have a higher rejection to anionic molecules [64,65].

3.4. Water permeability of composite membranes

The water permeability of polyester TFC membranes with different concentrations of ME monomer, different concentrations of NaOH and various IP times are shown in Fig. 5. As can be seen from Fig. 5**a**, for the different concentrations of ME monomer, the water permeability diminished from 87.13 to 11.79 LMH bar^{-1} by enhancing the ME concentration from 0.6 to 1.4 wt%. As confirmed by the SEM results (Fig. 3**e-h**), the thickness of the polyester selective films increased with the enhancement of the aqueous monomer concentration. This increase in the film thickness and high cross-linking degree caused by high monomer concentration results in a decrease of the water permeability.

It was found that enhancing the NaOH concentration from 0.35 to 0.55% improves the water permeability from 22.59 to 62.05 LMH bar^{-1} (Fig. 5**b**). Interestingly, a control membrane without the participation of NaOH was also prepared; it was found that no polyester film was formed after IP treatment. These results indicate that NaOH is indispensable in the formation of polyester films and has a pivotal impact on the formation of continuous polyester films. Topochemical degradation, derived from hydrolysis of aqueous NaOH, is a reaction that can lead to chain breaking of polyester compounds [66,67]. It is obvious that NaOH can reach any IP reactive zone where the ME monomers can diffuse. Therefore, we think that two processes of formation and hydrolysis of ester bonds are simultaneous, and that the balance between these two processes determines the bulk density of the polyester selective layer. The slow rates of hydrolysis allow for the formation of a continuous crosslinked polyester selective layer with a loose structure. Furthermore, by increasing the concentration of NaOH during the IP process, a much looser polyester film can be obtained, with improved permeability and decreased rejection of dyes/salts. (**see 3.5.1 and 3.5.2**).

As shown in Fig. 5c, the water permeability declined slightly from 54.4 to 41.1 when the reaction time increased from 1 to 4 min. Normally, changes in reaction time would have a significant effect on water permeability, but in this study there is a trade-off between the increased IP time (increased cross-linking degree) and sodium hydroxide hydrolysis (decreased cross-linking degree). The ester bonds, formed during IP, can be destroyed by hydroxide ions. Thus, IP and hydrolysis of ester bonds are occurring at the same time and the trade-off between them determines the slightly changed permeability of the resulting membrane [68].

3.5. Separation properties of composite membranes

3.5.1. Dye retention

Three different single dyes (CR, RB 2, DR 23) at 200 ppm were used to investigate the separation performance of polyester TFC LNF membranes. Fig. 6**a** manifests the effect of the ME concentration on the rejection and permeability of a dye solution. Increasing the ME concentration from 0.6 to 1.4 wt% improved the rejection of CR (98.97% to 99.46%), RB 2 (91.02% to 99.61%), and DR 23 (93.39% to 98.77%) but significantly decreases the permeability. The rejection of charged membranes is mainly determined by size sieving and the Donnan effect. As revealed by Fig. 4e-f, the higher the ME concentration that was used, the thicker the selective layer and the higher is the cross-linking degree, which results in a higher rejection of dyes, while lowering the permeability. In addition, the slight increase of electronegativity resulting from the increase of ME concentration, as shown in the zeta potential results, also contributes to the improvement of dye rejection. It was

reported that the highest rejection of CR (696.6 Da) than other dyes in this work is caused by the hydrophobic interaction between aromatic rings of adjacent dye molecules to form clusters or aggregates with large size [5]. It is interesting to note that with the increase of ME concentration, the rejection of reactive dye RB 2 is better than that of direct dye DR 23; this is possibly related to the low purity of DR 23 (dye content: > 30%). Furthermore, dyes existing in the form of aggregates and clusters in aqueous solution may also cause inconsistency between the rejection and the dyes molecular weight [69,70].

As shown in Fig. 6**b**, with increasing NaOH content from 0.35 to 0.55 wt%, the rejection of DR 23 decreased from 98.39% to 94.11%. As mentioned above (**3.4**), the topological hydrolysis reaction caused by the increase of NaOH content is strengthened and the final polyester structure is looser, thus leading to the decline of the dye rejection and the increased permeability. As displayed in Fig. 6c, the rejection of DR 23 increased slightly from 95.39% to 96.50% when the reaction time increased from 1 to 4 min. As the reaction time increased, the crosslinking density of polyester films increased, but it also means that the hydrolysis reaction is prolonged accordingly. Therefore, the IP time has little effect on rejection and permeability for a polyester TFC membrane made with NaOH catalyst due to the mutual limitation between the crosslinking reaction and the hydrolysis reaction.

3.5.2. Salt permeation

Sustainable development and saving resources (e.g., dye reuse and recycling the salts) is an important concept of modern textile wastewater treatment. Therefore, a loose nanofiltration membrane should be able to achieve a high salt permeability while effectively purifying the dye. Fig. 7 gives the single salt rejection (Na_2SO_4, NaCl) at 1 g/L and solution permeability of polyester TFC LNF membranes prepared under different conditions. The rejection of SO_4^{2-} is higher than that of Cl^{-1}, and all the membranes follow the salt rejection order of Na_2SO_4 > NaCl. Consistent with zeta potential results (Fig. 3**c**), this trend indicates that the surface of the polyester film is negatively charged. As shown in Fig. 7**a**, the rejection of Na_2SO_4 increased from 5.04% to 49.51% and the rejection of NaCl increased from 0% to 24.16% as the concentration of ME increased from 0.06 to 0.14 wt%. The increased rejection of Na_2SO_4 and NaCl was mainly caused by the increased crosslinking degree of polyester structure changes and the Donnan effect. According to the SEM results, the polyester film became thicker when a high concentration of ME was used. At high concentration, the aqueous monomer diffusion rate is higher, and the thickness and crosslinking degree of the polyester film are improved. In addition, as mentioned above, the membrane surface electronegativity increases slightly when the ME concentration increases. The increase in salt rejection of this polyester TFC LNF membrane is partly due to the higher electrostatic repulsion between the co-ions (SO_4^{2-}, Cl^-) and the membrane surface. The decreased water permeability from LNFM-1 to LNFM-5 primarily stems from the increased thickness and crosslinking degree of the polyester film.

Fig. 7**b** presents the salt rejection and water permeability of the polyester TFC LNF membranes prepared with different concentrations of NaOH. With increasing NaOH content from 0.35 to 0.55 wt%, the rejection of Na_2SO_4 decreased from 56.00% to 9.78% and the rejection of NaCl was decreased from 14.49% to 2.19%, while the permeability increased dramatically. As described in **3.4**, the increase in rejection and the decrease in permeability were mainly caused by the topochemical degradation of the polyester film caused by NaOH.

Fig. 7**c** shows the effect of different IP durations on the rejection and permeability of salt solutions. The rejection of Na_2SO_4 increased significantly from 15.60% to 59.14% and the rejection of NaCl increased slightly from 4.6% to 8.5% when the reaction time increased from 1 to 4 min.

Furthermore, some noteworthy phenomena can be observed in Fig. 7. The rejection of Na_2SO_4 changed significantly than NaCl with the change of membrane preparation conditions, which can be explained in terms of sieving and dielectric exclusion effects. The hydrated ionic radii of salts followed the order: sulfate (0.38 nm) > sodium (0.36 nm) > chloride (0.33 nm) [71]. That is one of the reasons that the rejection was higher for Na_2SO_4 than NaCl. Moreover, the selective layer of the prepared negatively charged polyester membrane may result in more electrostatic repulsion for bivalent co-ions (SO_4^{2-}) than monovalent ions (Cl^-) [72]. As a result, both the sieving effect and dielectric exclusion influenced the rejection of Na_2SO_4 more significantly than NaCl.

It can be seen from Table 3 that LNFM-1 is likely to meet the requirements of high permeability in practical applications, and LNFM-2 is more suitable when a higher dye rejection is needed. In order to further explain the antifouling, dye/salt separation and membrane stability performance, the LNFM-2 membrane was chosen in the following experiment.

3.5.3. Antifouling performance of composite membranes

Due to dye adsorption caused by the combination of hydrophobic impact, electrostatic interaction, van der Waals forces and hydrogen bonding, NF membranes are prone to membrane fouling in practical applications [12]. Ostuni et al. showed that the ideal anti-fouling membrane should have a good hydrophilicity, hydrogen bond receptors, and overall neutral properties [73]. The polyester TFC LNF membrane prepared from the ME monomer in this study has similar properties as above, so it may have an excellent anti-fouling performance. To investigate the anti-fouling performance of polyester TFC LNF membranes, three different types of dye solutions (DR 23, RB 2, CR) were selected as the sources of fouling. Fig. 8**a** presents the permeability of LNFM-2 membranes before and after dye filtration at 2 bar. After replacing deionized water with a dye solution, the permeability of polyester TFC LNF membranes decreased slightly. This was mainly caused by concentration polarization and membrane fouling. After rinsing with water, the permeability of the membranes contaminated with different dyes could recover to different levels. Finally, the

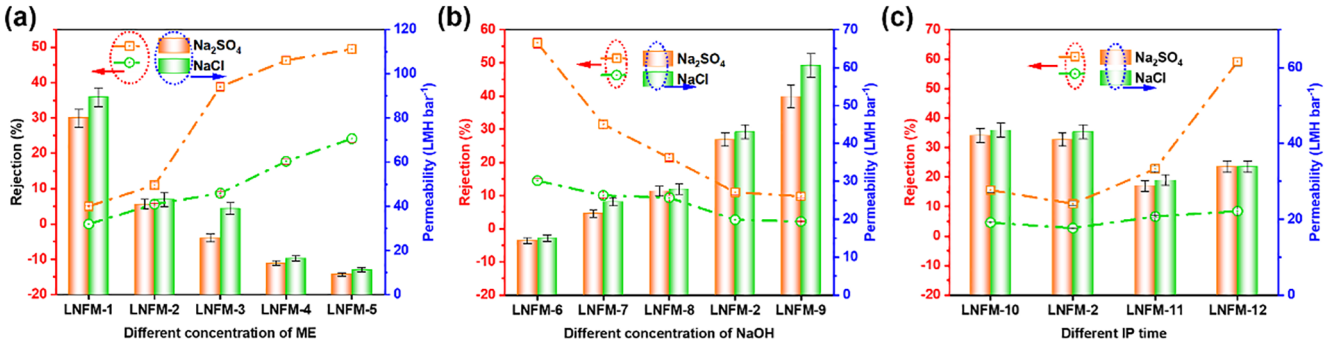

Fig. 7. Salt solution permeability and rejection of membranes with (a) different concentrations of ME monomer, (b) different concentrations of NaOH, (c) IP time (4 bar, 25 ± 3 °C).

Table 3
Comparison of dye/salt filtration performance.

Membrane	Method	Permeability (LMH bar^{-1})	Types of dye	Dye rejection (%)	Types of salts	Salt Rejection (%)	Ref
Catechol/PEI-$CuSO_4$/H_cO_2	Co-deposition	24.5	Congo red	99.75	Na_2SO_4	12.50	[21]
			Reactive black	99.69	NaCl	2.00	
			Methyl blue	99.3	$MgCl_2$	0.60	
					$MgSO_4$	7.50	
Tannic acid/PEI	Co-deposition	41.5	Congo red	99.5	Na_2SO_4	6.00	[22]
					NaCl	8.00	
EGCg/PEI	Co-deposition	19.0	Congo Red	99	Na_2SO_4	4.10	[19]
MoS_2-PSBMA/PES	Blending	18.5	Reactive black	98.20	Na_2SO_4	2.20	[24]
			Reactive green	99.30	NaCl	1.10	
					$MgCl_2$	1.20	
					$MgSO_4$	0.30	
GO-PSBMA/PES	Blending	11.98	Reactive black 5	99.20	Na_2SO_4	10.00	[6]
			Reactive red 49	97.20			
CS-MMT	Blending	15.6	Reactive black 5	95	Na_2SO_4	22	[12]
			Reactive red 49	87	NaCl	5	
Ag^+-PEI@HPAN	In situ self-assembly	10.6	Congo red	99.80	Na_2SO_4	12.80	[25]
			Acid fuchsin	99.50	NaCl	9.60	
			Crystal violet	99.20	$MgCl_2$	6.20	
					$MgSO_4$	8.30	
$Fe3^+$-PEI@HPAN	In situ self-assembly	6.0	Congo red	99.53	Na_2SO_4	5.89	[27]
			Methyl blue	99.92	NaCl	7.46	
			Acid fuchsin	98.99	$MgCl_2$	30.51	
			Crystal violet	92.86	$MgSO_4$	20.57	
Chitosan@HPAN	In situ self-assembly	7.2	Congo red	99.60	Na_2SO_4	4.80	[75]
			Acid fuchsin	98.70	NaCl	12.50	
TiO2-HMDI-PES/β-CD	In situ self-assembly	26.0	Congo red	97.4	Na_2SO_4	6.0	[76]
Membrane fouling		32.1	Direct red 80	99.9	NaCl	12.4	[20]
LNFM-1	IP	87.13	Congo red	98.97	Na_2SO_4	5.04	This work
			Direct red 23	93.39	NaCl	0	
			Reactive Blue 2	91.02			
LNFM-2	IP	53.23	Congo red	99.62	Na_2SO_4	11.00	This work
			Direct red 23	95.22	NaCl	5.60	
			Reactive Blue 2	99.55			

recovery of the permeability was calculated to evaluate the anti-fouling performance of the polyester TFC LNF membrane.

The flux recovery ratio (FRR) and fouling ratio of polyester TFC membranes are presented in Fig. 8**b**. The FRR value of polyester TFC membrane for three different dye solutions is around 90%, which indicates that the prepared polyester membrane has a superior anti-fouling performance. This indicates the good anti-fouling properties of the polyester TFC LNF membrane prepared with ME as monomer. In the best case, for the DR 23 solution, the FRR value of the membrane was 94.39%. This excellent anti-fouling performance is due to the combination of hydrophilic and electronegative properties of the polyester TFC LNF membrane. The hydrophilic surface can form a water layer by adsorbing water molecules, thereby hindering the adsorption of the dyes. In addition, the electrostatic repulsion between the negatively charged dyes and the negative surface also promotes improving the anti-fouling performance of the polyester TFC LNF membrane. The total fouling ratio (R_t) of polyester TFC LNF membrane, which is the sum of reversible fouling (R_r) and irreversible fouling (R_{ir}), is also shown in Fig. 8**b**. All R_{ir} values were below 11% for all three dye solutions. For DR 23, the R_{ir} value even reached as low as 5.61%. These results indicate that the polyester TFC LNF membranes exhibit excellent anti-fouling properties. In summary, the high FRR value and the low fouling ratio (R_t, R_r and R_{ir}) are the proofs of the excellent anti-fouling performance of the polyester TFC LNF membranes. This makes this type of ME-based TFC membranes highly competitive in the treatment of textile wastewater.

3.5.4. Effect of salt content in dye/salt filtration process

Na_2SO_4 was mixed with DR 23 (200 ppm) to prepare feed solutions with different salinities. As shown in Fig. 8**c**, with the increase of Na_2SO_4 concentration from 1 to 40 g/L at 200 ppm DR 23 solution, the permeability of the DR 23/Na_2SO_4 mixture slowly decreased from 37.99 to 30.30 HMH bar^{-1}, whereas the rejection of DR 23 remained almost constant (95.14% to 94.39%) and the rejection of Na_2CO_3 dropped from 7.80% to 0.06%. High salt contents can be coupled with charged dyes to enhance the dispersion of dye molecules [5]. However, uniformly dispersed dye molecules are easily adsorbed on the membrane pore wall, which leads to pore blocking, resulting in a decrease of the permeability [3,74]. On the other hand, concentration polarization on the membrane surface could increase with the salt concentration, resulting in a lower salt rejection. It is worth noting that the polyester TFC LNF membrane can maintain a high rejection against DR 23 (94.39%) and permeation for Na_2SO_4 (99.94%) at a high concentration of Na_2SO_4 (40 g/L).

The rejections of DR 23 and Na_2SO_4 remained constant except for some tiny fluctuations in the presence of Na_2SO_4 in the aqueous solution of DR23.

3.5.5. Stability of polyester membrane in dye/salt filtration

Fig. 8**d** shows the performance of the LNFM-2 membrane for purifying a DR 23/Na_2SO_4 mixture for 5 h continuous filtration at 2 bar. At the beginning, the permeability decreased from above 43 LMH bar^{-1} due to the influence of membrane fouling. However, under the influence of a excellent hydrophilicity and a looser polyester active layer of LNFM-2 membrane, the permeability remained at a high level (> 35 LMH bar^{-1}). Except for slight fluctuations in Na_2SO_4 rejection during the filtration process, the rejection of DR 23 and Na_2SO_4 was overall constant. After filtration for 5 h, the rejection of DR 23 and Na_2SO_4 was nearly 95.45 and 10%, respectively. Thus, the polyester TFC LNF membrane was found to have a extraordinary stability and fractionation ability in the separation of dye/salt mixtures.

Fig. 9 and Table 3 summarize a comparison of the dye/salt filtration performance of state-of-the-art loose NF membranes to that of the membranes prepared by different methods (co-deposition, blending, in situ self-assembly). It was obvious that both LNFM-1 and LNFM-2 exhibited a competitive performance. Compared with established loose

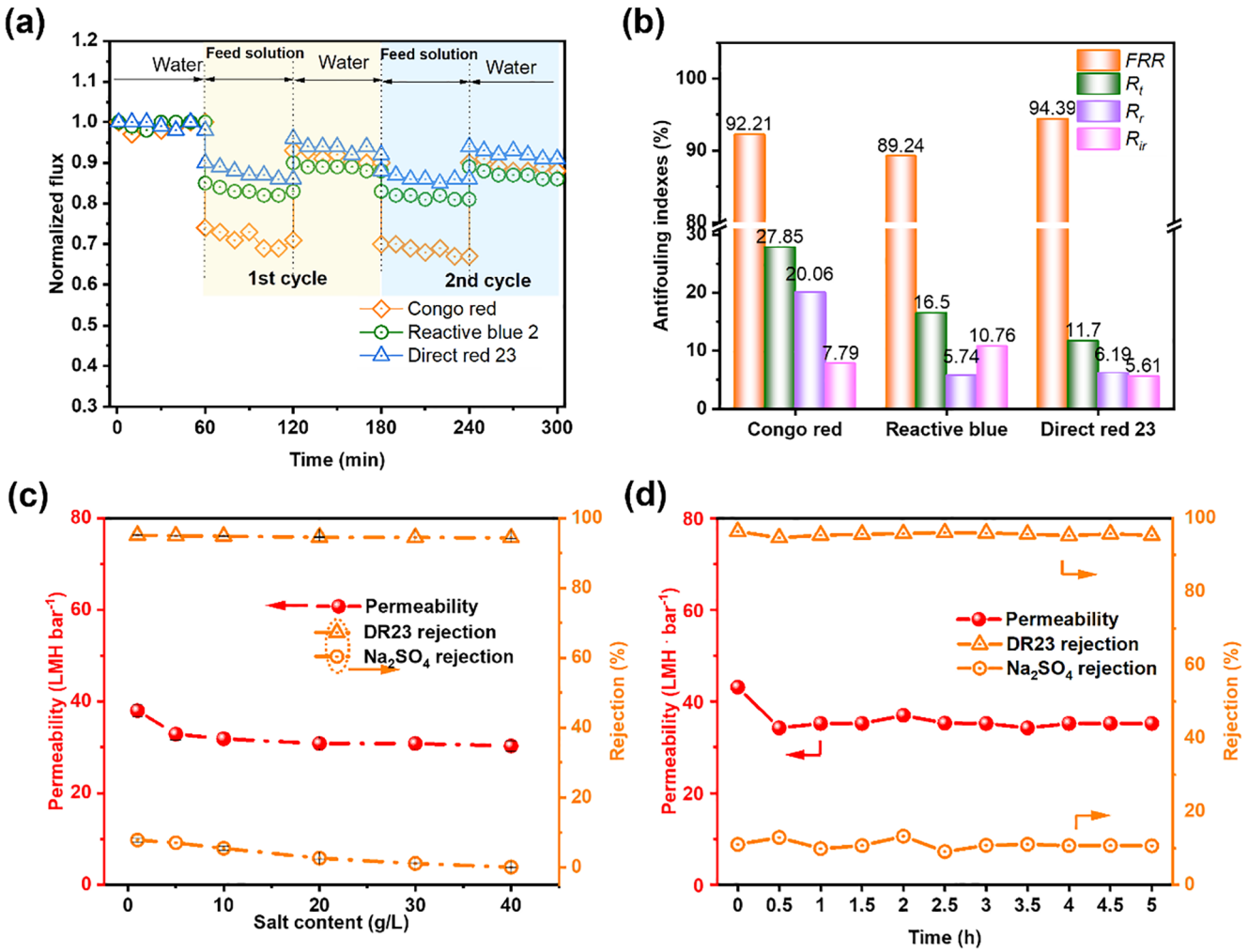

Fig. 8. (a) Normalized flux of LNFM-2 membrane before and after the filtration of Congo red, reactive blue 2 and direct red 23 solution separately and (b) fouling resistance ratio of LNFM-2 membrane; (c) effect of salt content on filtration performance of dye/salt mixture solution; (d) short-term stability of the prepared polyester LNF membrane, o.2 g/L DR 23 + 1 g/L Na_2SO_4. (For interpretation of the references to colour in this figure legend, the reader is referred to the web version of this article.)

NF membranes reported in the literature, the membrane in this work exhibited the highest permeability (87.13 LMH bar^{-1} for LNFM-1, 53.23 LMH bar^{-1} for LNFM-2 membrane) and a comparable fractionation of dye/salt mixtures. The high permeability, effective removal of dyes, high permeation of salts demonstrates that the polyester TFC LNF membrane prepared by interfacial polymerization can be regarded as promising alternative in real applications for textile wastewater.

4. Conclusions

A high-flux polyester LNF membrane was fabricated through an IP technique on PES support membranes with ME and TMC serving as the aqueous and organic monomers, respectively. The aqueous monomer of ME with low active hydroxyl groups played an important role in the IP reaction for preparing a polyester thin film with loose structure. The influence of preparation parameters on the separation performance of the polyester TFC membranes was comprehensively investigated. The optimized membrane yielded a remarkable water permeability (53.23 LMH bar^{-1}), dye rejection (CR, 99.62%; DR23, 95.22%; RB2, 99.55%) and salt permeation (Na_2SO_4, 89.00% and NaCl, 94.40%). Even in high salinity wastewater, the polyester TFC membrane can still maintain a high dye rejection and high salt permeation. In addition, the resultant membrane had an excellent stability and antifouling ability. This study not only proves that the method of interfacial polymerization can be used for preparing LNF membranes, but also suggests the use of other monomers with hydroxyl groups to make high-flux polyester LNF membranes for the treatment of textile wastewater.

Declaration of Competing Interest

The authors declare that they have no known competing financial interests or personal relationships that could have appeared to influence the work reported in this paper.

Acknowledgements

Pengrui Jin would like to acknowledge the support provided by China Scholarship Council (CSC) of the Ministry of Education, P.R. China (CSC No. 201806050043). The authors are grateful to National Nature Science Foundation of China (NSFC-21304060).

Appendix A. Supplementary data

Supplementary data to this article can be found online at https://doi.org/10.1016/j.cej.2020.126796.

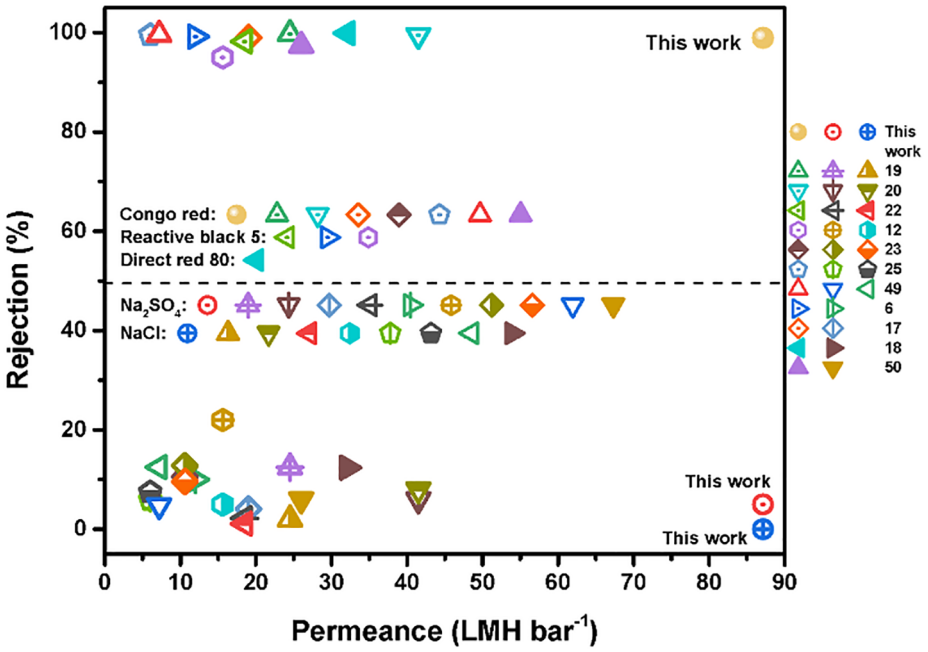

Fig. 9. Comparison of the polyester membrane with various lab made LNF membranes reported for dye desalination (for details see Table 3).

References

[1] G. Crini, P.-M. Badot, Application of chitosan, a natural aminopolysaccharide, for dye removal from aqueous solutions by adsorption processes using batch studies: a review of recent literature, Prog. Polym. Sci. 33 (2008) 399–447.

[2] V. Katheresan, J. Kansedo, S.Y. Lau, Efficiency of various recent wastewater dye removal methods: a review, J. Environ. Chem. Eng. 6 (2018) 4676–4697.

[3] L. Wang, N. Wang, G. Zhang, S. Ji, Covalent crosslinked assembly of tubular ceramic-based multilayer nanofiltration membranes for dye desalination, AIChE J. 59 (2013) 3834–3842.

[4] I. De Vreese, B. Van der Bruggen, Cotton and polyester dyeing using nanofiltered wastewater, Dyes Pigm. 74 (2007) 313–319.

[5] J. Lin, W. Ye, H. Zeng, H. Yang, J. Shen, S. Darvishmanesh, P. Luis, A. Sotto, B. Van der Bruggen, Fractionation of direct dyes and salts in aqueous solution using loose nanofiltration membranes, J. Membr. Sci. 477 (2015) 183–193.

[6] J. Zhu, M. Tian, J. Hou, J. Wang, J. Lin, Y. Zhang, J. Liu, B. Van der Bruggen, Surface zwitterionic functionalized graphene oxide for a novel loose nanofiltration membrane, J. Mater. Chem. A 4 (2016) 1980–1990.

[7] T.W. Seow, C.K. Lim, Removal of dye by adsorption: a review, Int. J. Appl. Eng. Res. 11 (2016) 2675–2679.

[8] M. Rochkind, S. Pasternak, Y. Paz, Using dyes for evaluating photocatalytic properties: a critical review, Molecules 20 (2015) 88–110.

[9] B. Bethi, S.H. Sonawane, B.A. Bhanvase, S.P. Gumfekar, Nanomaterials-based advanced oxidation processes for wastewater treatment: a review, Chem. Eng. Process. Process Intensif. 109 (2016) 178–189.

[10] G. Han, T.-S. Chung, M. Weber, C. Maletzko, Low-pressure nanofiltration hollow fiber membranes for effective fractionation of dyes and inorganic salts in textile wastewater, Environ. Sci. Technol. 52 (2018) 3676–3684.

[11] D. Ji, C. Xiao, S. An, J. Zhao, J. Hao, K. Chen, Preparation of high-flux PSF/GO loose nanofiltration hollow fiber membranes with dense-loose structure for treating textile wastewater, Chem. Eng. J. 363 (2019) 33–42.

[12] J. Zhu, M. Tian, Y. Zhang, H. Zhang, J. Liu, Fabrication of a novel “loose” nanofiltration membrane by facile blending with Chitosan-Montmorillonite nanosheets for dyes purification, Chem. Eng. J. 265 (2015) 184–193.

[13] P. Jin, S. Yuan, G. Zhang, J. Zhu, J. Zheng, P. Luis, B. Van der Bruggen, Polyarylene thioether sulfone/sulfonated sulfone nanofiltration membrane with enhancement of rejection and permeability via molecular design☆, J. Membr. Sci. 608 (2020) 118241.

[14] J.H. Huang, X.Q. Cheng, Y. Zhang, K. Wang, H. Liang, P. Wang, J. Ma, L. Shao, Polyelectrolyte grafted MOFs enable conjugated membranes for molecular separations in dual solvent systems, Cell Rep. Phys. Sci. 1 (2020) 100034.

[15] W. Deen, Hindered transport of large molecules in liquid-filled pores, AIChE J. 33 (1987) 1409–1425.

[16] F.G. Donnan, Theory of membrane equilibria and membrane potentials in the presence of non-dialysing electrolytes. A contribution to physical-chemical physiology, J. Membr. Sci. 100 (1995) 45–55.

[17] B. Van der Bruggen, E. Curcio, E. Drioli, Process intensification in the textile industry: the role of membrane technology, J. Environ. Manage. 73 (2004) 267–274.

[18] W. Ye, J. Lin, R. Borrego, D. Chen, A. Sotto, P. Luis, M. Liu, S. Zhao, C.Y. Tang, B. Van der Bruggen, Advanced desalination of dye/NaCl mixtures by a loose nanofiltration membrane for digital ink-jet printing, Sep. Purif. Technol. 197 (2018) 27–35.

[19] N. Zhang, B. Jiang, L. Zhang, Z. Huang, Y. Sun, Y. Zong, H. Zhang, Low-pressure electroneutral loose nanofiltration membranes with polyphenol-inspired coatings for effective dye/divalent salt separation, Chem. Eng. J. 359 (2019) 1442–1452.

[20] L. Shen, P. Li, T. Zhang, Green and feasible fabrication of loose nanofiltration membrane with high efficiency for fractionation of dye/NaCl mixture by taking advantage of membrane fouling, J. Appl. Polym. Sci. 136 (2019) 47438.

[21] J. Wang, R. He, X. Han, D. Jiao, J. Zhu, F. Lai, X. Liu, J. Liu, Y. Zhang, B. Van der Bruggen, High performance loose nanofiltration membranes obtained by a catechol-based route for efficient dye/salt separation, Chem. Eng. J. 121982 (2019).

[22] Q. Li, Z. Liao, X. Fang, D. Wang, J. Xie, X. Sun, L. Wang, J. Li, Tannic acid-polyethyleneimine crosslinked loose nanofiltration membrane for dye/salt mixture separation, J. Membr. Sci. 584 (2019) 324–332.

[23] W. Ye, K. Ye, F. Lin, H. Liu, M. Jiang, J. Wang, R. Liu, J. Lin, Enhanced fractionation of dye/salt mixtures by tight ultrafiltration membranes via fast bio-inspired co-deposition for sustainable textile wastewater management, Chem. Eng. J. 379 (2020) 122321.

[24] X. Liang, P. Wang, J. Wang, Y. Zhang, W. Wu, J. Liu, B. Van der Bruggen, Zwitterionic functionalized MoS2 nanosheets for a novel composite membrane with effective salt/dye separation performance, J. Membr. Sci. 573 (2019) 270–279.

[25] S. Liu, Z. Wang, M. Ban, P. Song, X. Song, B. Khan, Chelation–assisted in situ self-assembly route to prepare the loose PAN–based nanocomposite membrane for dye desalination, J. Membr. Sci. 566 (2018) 168–180.

[26] J. Zhang, L. Yang, Z. Wang, S. Yang, P. Li, P. Song, M. Ban, A highly permeable loose nanofiltration membrane prepared via layer assembled in-situ mineralization, J. Membr. Sci. (2019).

[27] P. Li, Z. Wang, L. Yang, S. Zhao, P. Song, B. Khan, A novel loose-NF membrane based on the phosphorylation and cross-linking of polyethyleneimine layer on porous PAN UF membranes, J. Membr. Sci. 555 (2018) 56–68.

[28] A.W. Mohammad, Y. Teow, W. Ang, Y. Chung, D. Oatley-Radcliffe, N. Hilal, Nanofiltration membranes review: Recent advances and future prospects, Desalination 356 (2015) 226–254.

[29] Z. Tan, S. Chen, X. Peng, L. Zhang, C. Gao, Polyamide membranes with nanoscale Turing structures for water purification, Science 360 (2018) 518–521.

[30] K.P. Lee, G. Bargeman, R. de Rooij, A.J. Kemperman, N.E. Benes, Interfacial polymerization of cyanuric chloride and monomeric amines: pH resistant thin film composite polyamine nanofiltration membranes, J. Membr. Sci. 523 (2017) 487–496.

[31] A. Akbari, E. Aliyarizadeh, S.M.M. Rostami, M. Homayoonfal, Novel sulfonated polyamide thin-film composite nanofiltration membranes with improved water flux and anti-fouling properties, Desalination 377 (2016) 11–22.

[32] J. Xu, H. Yan, Y. Zhang, G. Pan, Y. Liu, The morphology of fully-aromatic polyamide separation layer and its relationship with separation performance of TFC membranes, J. Membr. Sci. 541 (2017) 174–188.

[33] P. Arribas, M.C. García-Payo, M. Khayet, L. Gil, Improved antifouling performance of polyester thin film nanofiber composite membranes prepared by interfacial polymerization, J. Membr. Sci. 598 (2020) 117774.

[34] J. Cheng, W. Shi, L. Zhang, R. Zhang, A novel polyester composite nanofiltration membrane formed by interfacial polymerization of pentaerythritol (PE) and trimesoyl chloride (TMC), Appl. Surf. Sci. 416 (2017) 152–159.

[35] M.A. Seman, M. Khayet, N. Hilal, Nanofiltration thin-film composite polyester polyethersulfone-based membranes prepared by interfacial polymerization, J.

Membr. Sci. 348 (2010) 109–116.
[36] B. Tang, Z. Huo, P. Wu, Study on a novel polyester composite nanofiltration membrane by interfacial polymerization of triethanolamine (TEOA) and trimesoyl chloride (TMC): I. Preparation, characterization and nanofiltration properties test of membrane, J. Membr. Sci. 320 (2008) 198–205.
[37] M.A. Seman, M. Khayet, N. Hilal, Development of antifouling properties and performance of nanofiltration membranes modified by interfacial polymerisation, Desalination 273 (2011) 36–47.
[38] Y. Zhang, Y. Su, J. Peng, X. Zhao, J. Liu, J. Zhao, Z. Jiang, Composite nanofiltration membranes prepared by interfacial polymerization with natural material tannic acid and trimesoyl chloride, J. Membr. Sci. 429 (2013) 235–242.
[39] C. Zhou, Y. Shi, C. Sun, S. Yu, M. Liu, C. Gao, Thin-film composite membranes formed by interfacial polymerization with natural material sericin and trimesoyl chloride for nanofiltration, J. Membr. Sci. 471 (2014) 381–391.
[40] G. Odian, Principles of Polymerization, John Wiley & Sons, 2004.
[41] W. Zhao, H. Liu, N. Meng, M. Jian, H. Wang, X. Zhang, Graphene oxide incorporated thin film nanocomposite membrane at low concentration monomers, J. Membr. Sci. 565 (2018) 380–389.
[42] R. Zhang, S. Yu, W. Shi, W. Wang, X. Wang, Z. Zhang, L. Li, B. Zhang, X. Bao, A novel polyesteramide thin film composite nanofiltration membrane prepared by interfacial polymerization of serinol and trimesoyl chloride (TMC) catalyzed by 4-dimethylaminopyridine (DMAP), J. Membr. Sci. 542 (2017) 68–80.
[43] J. Xue, Z. Jiao, R. Bi, R. Zhang, X. You, F. Wang, L. Zhou, Y. Su, Z. Jiang, Chlorine-resistant polyester thin film composite nanofiltration membranes prepared with β-cyclodextrin, J. Membr. Sci. 584 (2019) 282–289.
[44] G.J. den Hartog, A.W. Boots, A. Adam-Perrot, F. Brouns, I.W. Verkooijen, A.R. Weseler, G.R. Haenen, A. Bast, Erythritol is a sweet antioxidant, Nutrition 26 (2010) 449–458.
[45] M.A. Aoki, G.M. Pastore, Y.K. Park, Microbial transformation of sucrose and glucose to erythritol, Biotechnol. Lett. 15 (1993) 383–388.
[46] W. Li, C. Bian, C. Fu, A. Zhou, C. Shi, J. Zhang, A poly (amide-co-ester) nanofiltration membrane using monomers of glucose and trimesoyl chloride, J. Membr. Sci. 504 (2016) 185–195.
[47] J. Liu, D. Hua, Y. Zhang, S. Japip, T.S. Chung, Precise molecular sieving architectures with janus pathways for both polar and nonpolar molecules, Adv. Mater. 30 (2018) 1705933.
[48] M.F. Jimenez-Solomon, Q. Song, K.E. Jelfs, M. Munoz-Ibanez, A.G. Livingston, Polymer nanofilms with enhanced microporosity by interfacial polymerization, Nat. Mater. 15 (2016) 760.
[49] R. Rautenbach, T. Linn, L. Eilers, Treatment of severely contaminated waste water by a combination of RO, high-pressure RO and NF — potential and limits of the process, J. Membr. Sci. 174 (2000) 231–241.
[50] C. Visvanathan, B.D. Marsono, B. Basu, Removal of THMP by nanofiltration: Effects of interference parameters, Water Res. 32 (1998) 3527–3538.
[51] T. Puspasari, N. Pradeep, K.-V. Peinemann, Crosslinked cellulose thin film composite nanofiltration membranes with zero salt rejection, J. Membr. Sci. 491 (2015) 132–137.
[52] Y. Mo, A. Tiraferri, N.Y. Yip, A. Adout, X. Huang, M. Elimelech, Improved Antifouling Properties of Polyamide Nanofiltration Membranes by Reducing the Density of Surface Carboxyl Groups, Environ. Sci. Technol. 46 (2012) 13253–13261.
[53] P. Arribas, M.d.C. García-Payo, M. Khayet, L. Gil, Improved antifouling performance of polyester thin film nanofiber composite membranes prepared by interfacial polymerization, J. Membr. Sci. 598 (2020) 117774.
[54] Y. Song, P. Sun, L.L. Henry, B. Sun, Mechanisms of structure and performance controlled thin film composite membrane formation via interfacial polymerization process, J. Membr. Sci. 251 (2005) 67–79.
[55] J. Zhu, J. Hou, R. Zhang, S. Yuan, J. Li, M. Tian, P. Wang, Y. Zhang, A. Volodin, B. Van der Bruggen, Rapid water transport through controllable, ultrathin polyamide nanofilms for high-performance nanofiltration, J. Mater. Chem. A 6 (2018) 15701–15709.
[56] J.S. Trivedi, D.V. Bhalani, G.R. Bhadu, S.K. Jewrajka, Multifunctional amines enable the formation of polyamide nanofilm composite ultrafiltration and nanofiltration membranes with modulated charge and performance, J. Mater. Chem. A 6 (2018) 20242–20253.
[57] B.-Q. Huang, Y.-J. Tang, Z.-X. Zeng, Z.-L. Xu, Microwave heating assistant preparation of high permselectivity polypiperazine-amide nanofiltration membrane during the interfacial polymerization process with low monomer concentration, J. Membr. Sci. 596 (2020) 117718.
[58] S. Karan, Z. Jiang, A.G. Livingston, Sub–10 nm polyamide nanofilms with ultrafast solvent transport for molecular separation, Science 348 (2015) 1347–1351.
[59] V. Freger, Kinetics of film formation by interfacial polycondensation, Langmuir 21 (2005) 1884–1894.
[60] J.-J. Wang, H.-C. Yang, M.-B. Wu, X. Zhang, Z.-K. Xu, Nanofiltration membranes with cellulose nanocrystals as an interlayer for unprecedented performance, J. Mater. Chem. A 5 (2017) 16289–16295.
[61] J. Zhu, S. Yuan, A. Uliana, J. Hou, J. Li, X. Li, M. Tian, Y. Chen, A. Volodin, B. Van der Bruggen, High-flux thin film composite membranes for nanofiltration mediated by a rapid co-deposition of polydopamine/piperazine, J. Membr. Sci. 554 (2018) 97–108.
[62] J. Zhu, S. Yuan, A. Uliana, J. Hou, J. Li, X. Li, M. Tian, Y. Chen, A. Volodin, B.V. der Bruggen, High-flux thin film composite membranes for nanofiltration mediated by a rapid co-deposition of polydopamine/piperazine, J. Membr. Sci. 554 (2018) 97–108.
[63] R.J. Petersen, Composite reverse osmosis and nanofiltration membranes, J. Membr. Sci. 83 (1993) 81–150.
[64] Y. Zhang, J. Ma, L. Shao, Ultra-thin trinity coating enabled by competitive reactions for unparalleled molecular separations, J. Mater. Chem. A (2020).
[65] Y. Zhang, X. Cheng, X. Jiang, J.J. Urban, C.H. Lau, S. Liu, L. Shao, Robust natural nanocomposites realizing unprecedented ultrafast precise molecular separations, Mater. Today (2020).
[66] M.S. Ellison, L.D. Fisher, K.W. Alger, S.H. Zeronian, Physical properties of polyester fibers degraded by aminolysis and by alkalin hydrolysis, J. Appl. Polym. Sci. 27 (1982) 247–257.
[67] J. Dave, R. Kumar, H.C. Srivastava, Studies on modification of polyester fabrics I: Alkaline hydrolysis, J. Appl. Polym. Sci. 33 (1987) 455–477.
[68] L.F. Villalobos, T. Huang, K.V. Peinemann, Cyclodextrin films with fast solvent transport and shape-selective permeability, Adv. Mater. 29 (2017) 1606641.
[69] J. Lin, W. Ye, M.-C. Baltaru, Y.P. Tang, N.J. Bernstein, P. Gao, S. Balta, M. Vlad, A. Volodin, A. Sotto, P. Luis, A.L. Zydney, B. Van der Bruggen, Tight ultrafiltration membranes for enhanced separation of dyes and Na2SO4 during textile wastewater treatment, J. Membr. Sci. 514 (2016) 217–228.
[70] J. Zhu, A. Uliana, J. Wang, S. Yuan, J. Li, M. Tian, K. Simoens, A. Volodin, J. Lin, K. Bernaerts, Elevated salt transport of antimicrobial loose nanofiltration membranes enabled by copper nanoparticles via fast bioinspired deposition, J. Mater. Chem. A 4 (2016) 13211–13222.
[71] J. Schaep, B. Van der Bruggen, C. Vandecasteele, D. Wilms, Influence of ion size and charge in nanofiltration, Sep. Purif. Technol. 14 (1998) 155–162.
[72] S. Zhao, Z. Wang, A loose nano-filtration membrane prepared by coating HPAN UF membrane with modified PEI for dye reuse and desalination, J. Membr. Sci. 524 (2017) 214–224.
[73] E. Ostuni, R.G. Chapman, R.E. Holmlin, S. Takayama, G.M. Whitesides, A survey of structure−property relationships of surfaces that resist the adsorption of protein, Langmuir 17 (2001) 5605–5620.
[74] P. Chen, X. Ma, Z. Zhong, F. Zhang, W. Xing, Y. Fan, Performance of ceramic nanofiltration membrane for desalination of dye solutions containing NaCl and Na2SO4, Desalination 404 (2017) 102–111.
[75] S. Liu, Z. Wang, P. Song, Free radical graft copolymerization strategy to prepare catechin-modified chitosan loose nanofiltration (NF) membrane for dye desalination, ACS Sustainable Chem. Eng. 6 (2018) 4253–4263.
[76] L. Zhang, H. Guan, N. Zhang, B. Jiang, Y. Sun, N. Yang, A loose NF membrane by grafting TiO2-HMDI nanoparticles on PES/β-CD substrate for dye/salt separation, Sep. Purif. Technol. 218 (2019) 8–19.